jet INTL JOURNAL OF ELECTRONICS AND TELECOMMUNICATIONS, 2011, VOL. 57, NO. 4, PP. 433–436
Manuscript received September 29, 2011; revised November 2011. DOI: 10.2478/v10177-011-0059-y

The ISAR Image Post-Processing for Multi-Point Target Identification

Maxim Konovalyuk, Anastasia Gorbunova, Yury Kuznetsov, and Andrey Baev

***Abstract*—The wideband coherent pulse radar provides high resolution image of the target. A model of this image is composed of the complex envelope superposition of signals diffracted by the point scatterers. The values of complex envelope are distributed over the radar image coordinate plane in accordance with the point scatterer's positions and their reflection coefficients. The radar image model is combining of the range and Doppler profiles. The parameters of the target point scatterers are processed using one dimensional data extracted from the complex discrete Fourier transform of the radar image. The proposed parametric system identification method performs estimation of signal model parameters for the short dwell time and extrapolation of the radar data outside this time. Also the procedure of the ISAR imaging based on the proposed algorithm is introduced. The reducing smeared Doppler shifts and improving image resolution are achieved as a result.**

***Keywords*—Radar image, dwell time, point scatterer, Doppler smearing, radar cross-range profile, resolution.**

I. Introduction

THE modern wideband radar systems allow target recognition and identification owing to their high range resolution [1]. High range resolution of a radar system makes it possible to get the information about the target's shape and geometrical dimensions, which may be used for the target identification. It is known that the response from a target on a short radar pulse may be described as a superposition of the responses from the point scatterers [2]. The information about the positional relationship of the most powerful scatterers of the target may be used for the determination of the target's shape and dimensions. According to the geometrical theory of electromagnetic back-scattering each object with an elementary shape like sphere, cone, the edge, and so on can be described by a single point-scatterer, situated on its surface in the phase center [3]. Each man-made target in the X-band can be represented as a superposition of the jointed primitive elements. So any man-made object can be uniquely described by its point-scatterer model.

The responses from the point scatterers may be considered as a signals reflected from them [4]. However, the distance between scattering centers may be far lesser than the radar range resolution, which considerably complicates the target recognition directly from its radar range profile. The implementation of the complex radar image technology requires the coherent pulse radar mode. The main reason for the using of the complex imaging technology in wideband radar systems is the necessity of the image resolution improving. The paper considers coherent X-band radar emitting a wideband signal in the form of a sequence of short pulses without chirp modulation. In this case the overlapped over several resolution elements range profile of the target can be obtained due to the pulse duration. It is also assumed the radar with a non-scanning antenna system having a beam width much larger than the target angular dimension [5].

The resolution of the radar target image along the cross-range is determined by the resolution along Doppler frequency shift. Consequently, in order to improve the cross-range resolution, observation time should be increased [6]. However, it should be taken into account that the motion of a point scatterer on the target is rectilinear and uniform on a short interval of observation time only, therefore, radial component of the speed varies with the increasing of the observation time, which causes Doppler spectrum smearing.

This work was supported by Russian Foundation for Basic Research, Grant No. 11-07-00029-a.l

M. Konovalyuk, A. Gorbunova, Y. Kuznetsov, and A. Baev are with Theoretical Radio Engineering Department, Moscow Aviation Institute (State Technical University), Moscow, Russia (e-mail: mai@mai-trt).

II. Radar Image Model

The complex envelope of a radar signal reflected from P point scatterers of the moving target can be expressed as

$$\dot{x}(t) = \sum_{p=1}^{P} \dot{A}_p \cdot \dot{s}[t - \tau_p(t)] = \sum_{p=1}^{P} \dot{A}_p \cdot \dot{s}[t - 2\rho_p(t)/c] \quad (1)$$

where $\dot{s}(t) = \sum_{n=0}^{N-1} \dot{s}_0(t - nT)$ is a complex envelope of a signal composed of N radar transmitted pulses $\dot{s}_0(t)$; T is a pulse period; $\dot{A}_p$ is a complex amplitude of the signal reflected from the p-th scatterer; $\tau_p(t)$ is a round-trip delay proportional to the time-varying range $\rho_p(t)$ from the radar to the p-th scatterer; c is a speed of electromagnetic wave propagation.

In assumption of a short observation time $\Delta T = NT$, during which the radial velocity variation for each scatterer on the target can be neglected, it can be represented as:

$$v_p(t) = \frac{d\rho_p(t)}{dt} \cong v_{0p}, \quad p = 1, 2, \ldots, P. \quad (2)$$

The Doppler frequency shift for the p-th scatterer is determined by the expression:

$$f_{Dp} = f_0 \cdot \frac{2v_{0p}}{c} \quad (3)$$

where f_0 is a carrier frequency.

Figure 1 shows the scheme of radar emitting coherent pulse train and received radar signal in the form of buffered range

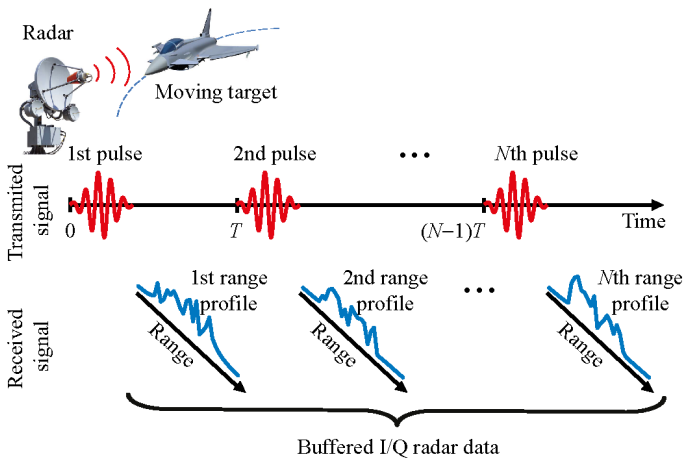

Fig. 1. Inverse synthetic aperture radar (ISAR) principle scheme, radar dwell and buffering radar data.

profiles. Each range profile consists of inphase and quadrature (I/Q) components as a result of quadrature detection of received radar signal.

The model of a digitized received radar signal can be expressed as follows:

$$\dot{y}[k] = \sum_{p=1}^{P} \sum_{m=0}^{M-1} \dot{A}_p \cdot \dot{s}_0(k\Delta t - \tau_p(k\Delta t) - mT) + \dot{w}[k], \quad (4)$$

$$k = 0, 1, 2, \ldots$$

where Δt is a time sampling interval; $\dot{w}[k]$ is a complex additive white Gaussian noise in the radar receiver bandwidth.

The spectrum of the N signal samples $\dot{y}[k]$ that are processed over one pulse period $T = N\Delta t$, may be described by a product of the radar pulse spectrum $\dot{S}_{0N}[n]$ and the exponential terms which are derived using the fixed ($\rho_p(t) \cong \rho_{0p}$, $0 \le t \le T$) point-scatterer model in the frequency domain:

$$\sum_{k=0}^{N-1} \dot{y}[k] \cdot e^{-j2\pi \frac{k}{N-1} n} = \dot{S}_{0N}[n] \cdot \left(\sum_{p=1}^{P} \dot{A}_p \cdot e^{-j \frac{2\pi}{\Delta t} \cdot \frac{n}{N-1} \cdot \tau_{0p}} \right) =$$

$$= \dot{S}_{0N}[n] \cdot \dot{D}_N[n], \quad n = 0, 1, \ldots, N-1, \quad (5)$$

where: $\tau_{0p} = \frac{2\rho_{0p}}{c}$.

The Doppler spectrum of the moving target can be represented as a set of harmonics with frequencies determined by the Doppler shifts of the scatterers on the target:

$$\sum_{k=0}^{N \cdot M-1} \dot{y}[k] \cdot e^{-j2\pi \frac{k}{N-1} \mu} =$$

$$= \sum_{m=0}^{M-1} \left(\sum_{p=1}^{P} \dot{A}_p \cdot e^{j2\pi f_{Dp} mT} \right) \cdot e^{-j2\pi \frac{m}{M-1} \mu} =$$

$$= \sum_{m=0}^{M-1} \dot{q}_M[m] \cdot e^{-j2\pi \frac{m}{M-1} \mu}, \quad \mu = 0, \pm 1, \ldots, \pm M/2. \quad (6)$$

During all coherent processing time interval $\Delta T = MT$ the M sequences by the N samples of the received signal

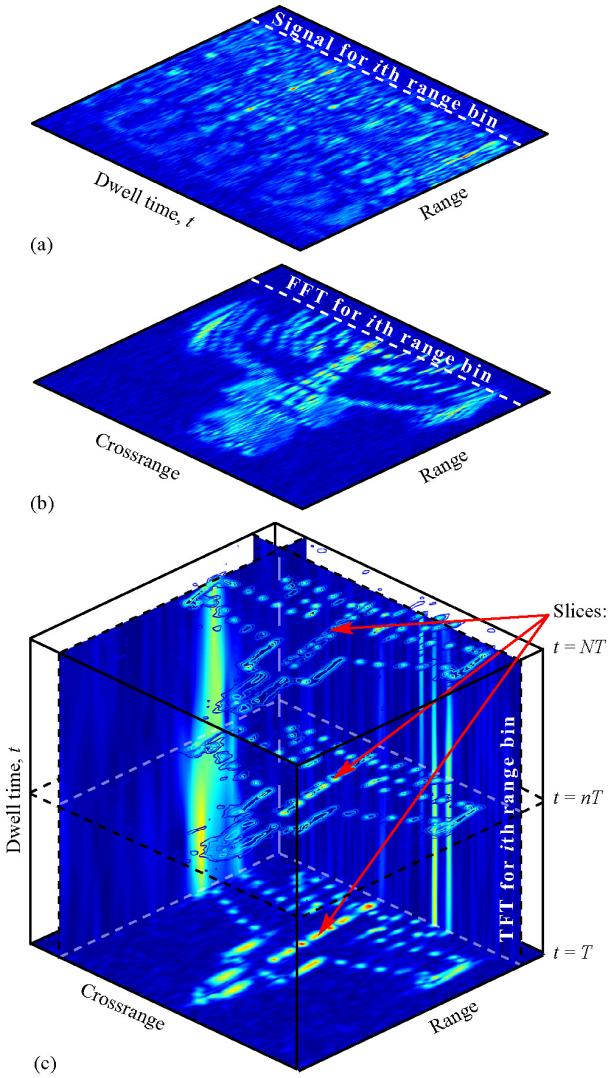

Fig. 2. Buffered ISAR data (a), ISAR image based on fast Fourier transform (FFT) (b), ISAR images as the slices of generated 3-D dimensional array using time-frequency transform (TFT) (c).

$\dot{y}[k]$ per pulse period $T = N\Delta t$ can be formed into the two dimensional $N \times M$ data (see Fig. 1a):

$$\dot{y}_{N \times M}[n, m] = \dot{y}[n - mN], \quad n = 0, 1, \ldots, N-1, \quad (7)$$

$$m = 0, 1, \ldots, M-1.$$

The radar image can be processed by the discrete or fast Fourier transform (FFT) of the N data rows (see Figure 2a):

$$\dot{z}(r_n, h_\mu) = \dot{z}_{N \times M}[n, \mu] = \sum_{m=0}^{M-1} \dot{y}_{N \times M}[n, m] \cdot e^{-j2\pi \frac{m}{M-1} \mu}. \quad (8)$$

Figure 2b shows the radar image which size is $N \times M$, in the range and cross-range plane. The image columns, which lengths are N, are radar range profiles. And the image rows which lengths are M, are radar Doppler profiles.

The radar range profile of a target contains information about the length of the target under observation along the line of sight and the locations of the scatterer's projections

TABLE I
COMPARISON OF DIFFERNNT RADAR IMAGING PROCEDURES

Radar Imaging Procedure	Windowing	Extrapolation	Resolution
FFT	no	no	1/*Data Length*
TFT	yes	no	$\sim$ 1/*Window Length*
Parametric Spectral Analysis	yes	yes	$\sim$ 1/*Data Length*

on this direction. The range resolution is determined by the pulse duration τ:

$$\Delta_r = \frac{2\tau}{c}. \tag{9}$$

Doppler shifts of the scattering centers are different in the case of the rotating target. The Doppler resolution is inversely proportional to the observation time ΔT. The Doppler shift is proportional to the cross-range of the scattering center with a scaling factor related to the radar wavelength λ and the rotation rate Ω of the target.

Thus, the cross-range resolution is determined as follows:

$$\Delta_h = \frac{\lambda}{2\Omega} \cdot \Delta_{f_D} = \frac{\lambda}{2\Omega \Delta T}. \tag{10}$$

III. RADAR IMAGE POST-PROCESSING

In order to enhance the resolution of the ISAR image, several methods can be applied. The one algorithm is based on the time-frequency transform of radar data along the dwell time. This algorithm was proposed as joint time frequency (JTF) analysis [3]. Each time-frequency transform of the data sequence is a 2 dimensional (2-D) signal. Such transforms are collected into array versus range. Finally the image formation is a sampling in dwell time and obtaining slices of 3 dimensional (3-D) array. Figure 2 shows that FFT algorithm produces image with blurring due to the rotation of the target. In the contrary JTF analysis allows to observe the time history of target motion. This can be represented as the movie with the slices of 3-D array instead of the frames.

We suggest another algorithm based on parametric approach of spectral analysis. The diagram of this alternative algorithm is shown in Figure 3. Primarily as shown in figure full dwell time data are divided into frames in order to minimize smearing. Therefore the image resolution is degraded. Then parametric identification method [4] can be applied to enhance the resolution of the radar image. In according to this method the parameters of the point scatterers such as the coordinates along cross-range and reflection coefficients are determined for each range bin. Finally we extrapolate the signal outside of the frames and process cross-range profiles of image using FFT.

This approach requires information about the model of the signal. Such appropriate mathematical model is a sum of the discrete complex exponents corrupted by complex additive white Gaussian noise (AWGN). The procedure of parametric spectral analysis is properly composed from two main operations which are executed sequentially [5]. These are model order selection and model parameter estimation

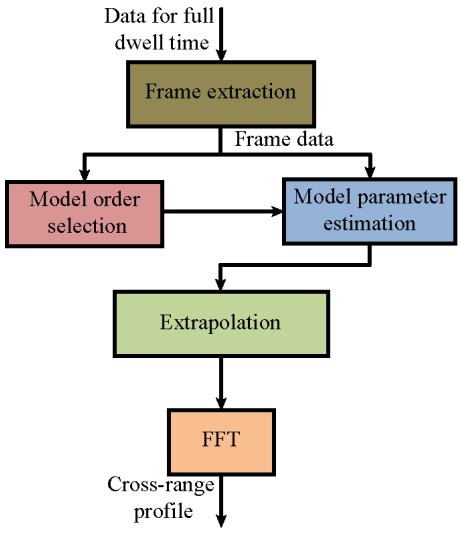

Fig. 3. Diagram of the parametric spectral analysis algorithm.

implemented using the information criteria [6] and the matrix pencil method [7] respectively.

Some obvious characteristics of discussed algorithms are presented in Table 1. We can analyze several features of JTF and procedure based on parametric spectral analysis. In both cases windowing is available to achieve least smearing. In the last procedure the extrapolation provides high resolution cross-range profiles with the resultant resolution approximately inversely proportional to the data length N for full dwell time as well as it can be achieved using FFT algorithm.

IV. SIMULATED RESULTS

In the following example ISAR simulated data were borrowed from the open source [8] and used for algorithm comparison purpose (see Figure 4). The radar image of aircraft MiG-25 can be processed using these data [9]. The data were simulated for more than 100 point scatterers. The initial test data were noised by complex value AWGN. The corresponding signal to noise ratio (SNR) was 5 dB.

There are the initial data, processed images using compared algorithms and corresponding two dimensional (2-D) signals shown in Figure 4. It can be seen signals and images in Figure 4a and Figure 4b respectively placed into 2×2 box. In the upper left corner each block is labeled with the letter and the number to match them to each other in the different boxes.

Figure 4c shows cross-range profiles which are different for the equal range bin. The dotted line corresponds to the FFT of initial data. The dash line passes through the profile generated with TFT using Gaussian window. The responses shown by the solid line are computed using FFT of windowed extrapolated signal (see Figure 4a, block a4) in the form of complex exponents with estimated parameters for frame data demonstrated above in block a2.

In the last case the time history of the image evolution could be demonstrated by the sequential processing of the other frames extracted from the full time dwell data as well as it allows JTF algorithm.

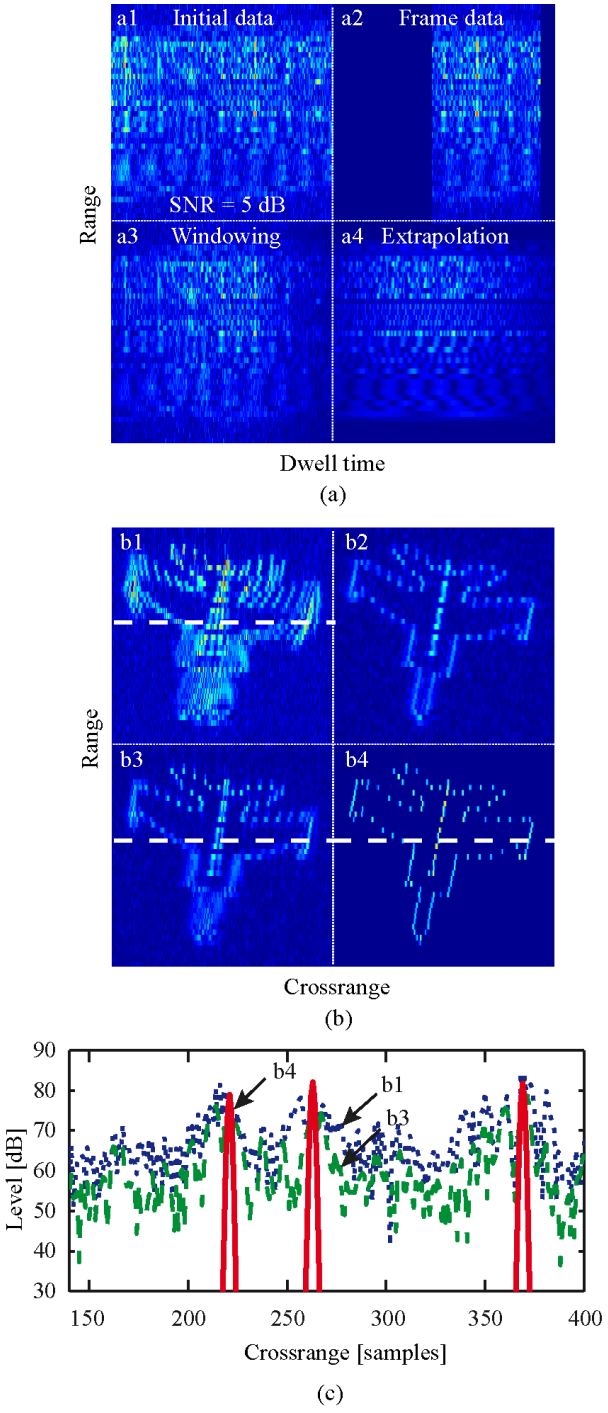

Fig. 4. Dwell time-domain data (a) and corresponding ISAR images (b) are comparing for different radar imaging procedures: 1) initial noisy data (SNR = 5 dB); 2) frame data; 3) TFT based approach with windowing (Gaussian); 4) parametric extrapolation of frame data; in crossections (c) over marking dash line.

V. Conclusion

The paper demonstrates suggested parametric identification for post-processing of the complex radar image. There are known ISAR radar image algorithms. Their difference lies in the selected type of the spectral analysis. FFT and TFT based algorithms use non-parametric approach. We used the parametric spectral analysis to estimate the model parameters and extrapolate radar data along the dwell time. In order to achieve the improving of radar image resolution significantly by image processing it is need to know prior information about model of the target radar portrait assuming the superposition of the identical partial responses from the target point-scatterers. Parametric methods of spectral estimation were applied to precisely determine parameters of the point scattering centers. The simulation example demonstrates improving the quality of radar image corrupted by noise. The analysis of imaging procedures based on their own distinctive features can be useful to select the most appropriate one in the given conditions of radar application.

References

[1] K. M. Cuomo, J. E. Piou, and J. T. Mayhan, "Ultra-Wideband Coherent Processing," *Lincoln Laboratory Journal*, vol. 10, no. 2, pp. 203–221, 1997.

[2] A. W. Rihaczek and S. J. Hershkowitz, *Theory and Practice of Radar Target Identification*. Artech House, 2000.

[3] V. C. Chen and H. Ling, *Time-Frequency Transforms for Radar Imaging and Signal Analysis*. Artech House, 2002.

[4] M. Konovaluk, Y. Kuznetsov, and A. Baev, "Point Scatterers Target Identification Using Frequency Domain Signal Processing," in *17th International Conference on Microwaves, Radar and Wireless Communications*, Wroclaw, Poland, May 2008, pp. 429–432.

[5] ——, "Moving Multy-Scatterer Target Parametric Identification Using Radar Image," in *18th International Conference on Microwaves, Radar and Wireless Communications MIKON-2010*, Vilnus, Lithuania, June 14–16 2010, pp. 524–527.

[6] A. Gorbunova and Y. Kuznetsov, "Model Order Selection of the Target Doppler Spectrum," in *18th International Conference on Microwaves, Radar and Wireless Communications MIKON-2010*, Vilnus, Lithuania, June 14–16 2010, pp. 776–779.

[7] T. K. Sarkar and O. Pereira, "Using the Matrix Pencil Method to Estimate the Parameters of a Sum of Complex Exponentials," *IEEE Antennas and Propagation Magazine*, vol. 37, no. 1, February 1995.

[8] V. C. Chen, 1999, [Online]. Available: http://airborne.nrl.navy.mil/ vchen/tftsa.html.

[9] J. M. Munoz-Ferreras and F. Perez-Martinez, "On the Doppler Spreading Effect for the Range-Instantaneous-Doppler Technique in Inverse Synthetic Aperture Radar Imagery," *IEEE Geoscience and Remote Sensing Letters*, vol. 7, no. 1, pp. 180–184, January 2010.